Journal of Power Sources 196 (2011) 9022–9026

Contents lists available at ScienceDirect

Journal of Power Sources

journal homepage: www.elsevier.com/locate/jpowsour

Short communication

Residual stress and redox cycling of segmented-in-series solid oxide fuel cells

K. Fujita*, T. Somekawa, T. Hatae, Y. Matsuzaki

Product Development Department, Tokyo Gas Co. Ltd., 3-13-1, Minami-senjyu, Arakawa-ku, Tokyo 116-0003, Japan

ARTICLE INFO

Article history:
Received 29 October 2010
Received in revised form
22 December 2010
Accepted 7 January 2011
Available online 19 January 2011

Keywords:
Solid oxide fuel cell
Redox
Segmented-in-series
Residual stress

ABSTRACT

Residual stresses in the electrolytes of segmented-in-series solid oxide fuel cells (SIS-SOFCs) and anode-supported cells (ASCs) were estimated at room temperature by X-ray diffraction. In the SIS-SOFCs, the residual stresses in the electrolyte were smaller than in the ASCs and did not change significantly after redox cycling. For both designs, numerically calculated values of the residual stresses in the electrolyte were found to be comparable to the experimental results. Next, in order to simulate the reoxidation reaction, the anode was subjected to forced expansion, and the residual stresses were estimated at high temperatures. It was found that in the SIS-SOFC, the dimensional changes and residual stresses were smaller than those in the ASC. The high redox tolerance of the SIS-SOFC is considered to stem from the fact that the electrically insulated substrate prevents the expansion and deformation of the positive electrode–electrolyte–negative electrode structure.

1. Introduction

The development of various solid oxide fuel cell (SOFC) systems has progressed steadily in recent years due to the successful performance they have demonstrated [1–3].

Practical use of SOFC systems for residential applications will require high redox tolerance to reach the necessary high efficiency with a simple fuel utilization control mechanism [4–6]. A high redox tolerance also offers other advantages such as a shutdown sequence without any reduction gases, which contribute to reliability.

However, the performance of anode-supported cells (ASCs) degrades with redox cycling because the anode expansion caused by micro-structural changes leads to the formation of cracks in the electrolyte [7]. Thus, in order to enhance the redox tolerance of SOFCs, micro-structural modification [8] of the anode, the use of an oxidation barrier layer [9], and the use of a new anode material $La_{0.75}Sr_{0.25}Cr_{0.5}Mn_{0.5}O_3$ [10] have been the subject of recent studies.

In addition, the mechanism responsible for performance degradation due to thermal cycling has been studied by measuring the residual stresses in the electrolyte using X-ray measurement methods [11] and numerical analysis [12,13]. The residual stresses are affected by the thicknesses of the anode, electrolyte, and cathode, and the positive electrode–electrolyte–negative electrode (PEN) structure has been optimized using a numerical model [14].

In segmented-in-series solid oxide fuel cells (SIS-SOFCs) [15–17], the anode layers, which are supported by an electrically insulating porous substrate, are thinner than in conventional ACSs. Fig. 1 shows schematic representations of the plane and cross-sectional views of typical SIS-SOFCs. The substrate shows high chemical stability and is characterized by qualities such as low dimensional changes and small structural changes [18–20]. We have measured the redox tolerance of an SIS-SOFC and found it to have a very low degradation rate [21].

In this paper, we report our evaluation of the residual stresses in the electrolyte of a SIS-SOFC during redox cycling on the basis of X-ray diffraction and numerical analyses, which reveal the effect of the thicknesses of the anode and substrate on residual stresses.

2. Experimental

2.1. Sample preparation

The SIS-SOFC is supported by an electrically insulating porous oxide material on which 16 single cells are arrayed electrically in series, as shown in Fig. 1. The substrate was prepared from a Ni-doped MgO-based material by extrusion in the form of a flattened tube. The anode was prepared using NiO powder (99.9%, Seido Chemical Industry Co., Ltd.) and 8 mol% YSZ powder (TZ-8Y, Toso Co., Ltd.). The anode sheets were produced using a tape casting method, and the sheets and substrate which were bonded with an organic solvent were dipped in a YSZ slurry. Next, the YSZ electrolyte and the anodes were co-fired with the substrate at 1500 °C for 2 h [18,19], and the cathode, which was prepared using Sr- and Co-doped $LaFeO_3$ (LSCF), was screen printed onto the

* Corresponding author. Tel.: +81 3 5604 8275; fax: +81 3 5604 8051.
E-mail address: k-fujita@tokyo-gas.co.jp (K. Fujita).

0378-7753/$ – see front matter © 2011 Elsevier B.V. All rights reserved.
doi:10.1016/j.jpowsour.2011.01.022

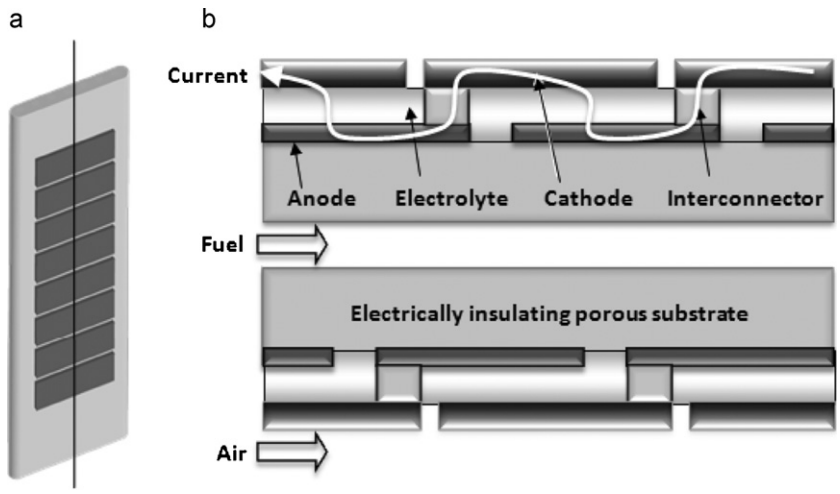

Fig. 1. Schematic representation of (a) plane view and (b) cross-sectional view of SIS-SOFC.

electrolyte and sintered at 1200 °C for 2 h. SIS-SOFCs of thickness ~3 mm, both with and without the anode function layer (AFL), were fabricated. The sample preparation details are reported elsewhere [15–19,22].

Two kinds of ASCs of different thicknesses were fabricated for the sake of comparison with the SIS-SOFCs. The anode of the Ni-YSZ was formed by the conventional press molding method and the YSZ electrolyte slurry was dipped in the anode substrate. The substrates with the dipped YSZ were co-fired and the cathode of LSCF was screen-printed onto the electrolyte [23,24]. ASCs with thicknesses of 3 mm and 0.5 mm were prepared for comparison with the thickness of the substrate and anode of the SIS-SOFC.

Reduced samples were obtained by sintering in a 4%H_2–N_2 atmosphere at 750 °C for 100 h, and the re-oxidation samples were prepared by annealing in air at 750 °C for 100 h. The redox samples were produced by repeating these redox cycles.

2.2. SEM images after redox cycling

The electrolyte surfaces of the SIS-SOFCs and ASCs after redox cycling were analysed using a scanning electron microscope (SEM, JEOL Ltd., JSM-6510A) to confirm the cracks on the electrolyte. When cracks were observed on the electrolyte surface, cross-sectional views of the samples were analysed.

2.3. X-ray residual stress measurement

The thermal stresses in the electrolyte of the SIS-SOFCs and ASCs were measured at room temperature using an X-ray diffractometer (Rigaku Co. Ltd., RINT-2000). The typical cell sizes were 30 mm × 30 mm, and the cathodes were removed from the electrolyte before the X-ray measurement. The residual stresses were estimated using the $\sin^2\Psi$ methods, and the Cu-$K\alpha$ X-ray source was selected. For the diffracting plane used for the stress measurements, we selected the (5 3 1) plane of 8YSZ.

The residual stresses in the electrolyte were estimated using the following formula.

$$\sigma = \frac{1}{d_0} \times \frac{E}{1+\nu} \times \frac{\partial d_\psi}{\partial \sin^2 \psi}$$

where d_0 is the inter-planar spacing under a stress free condition, and E and ν are the Young's modulus of 215 GPa and Poisson's ratio of 0.3, respectively, using data taken from previous reports [13,25,26].

2.4. Residual stress simulation

The residual thermal stresses in the SIS-SOFC and ASCs were simulated using the numerical finite element software COMSOL 3.5a (COMSOL AB, Sweden). The parameters of the electrolyte, anode, AFL, and substrate are listed in Table 1. These parameters were taken from Yakabe's residual stress simulation data [13] in order to validate our simulated results. The simulated sample geometry used was 10 mm × 10 mm, since it was reported that at 5 mm or more, the results are almost independent of the cell size [13]. Thus, we carried out the simulations in the range of a low size influence, and the co-firing temperature at which each component (anode, electrolyte, and substrate) was sintered was assumed to be 1400 °C. First, we calculated the residual thermal stress in each SOFC at 25 °C and confirmed the validity of the simulated results with those of previous reports.

Next, thermal stress at 750 °C, which is the SOFC operating temperature, was simulated, and the reoxidation effect upon the residual stress in each SOFC was assumed to result in anode expansion of 50 μm.

Table 1
Material properties of components in SIS-SOFC and ASC.

	Young's modulus (GPa)	Poisson's ratio	Thermal expansion coefficient ($\times 10^{-6}$ K^{-1})	Thickness (mm)
Electrolyte	207	0.3	10.56	0.05
Anode	96	0.3	12.22	ACS: 0.5, 3.0SIS-SOFC: 0.1
AFL	96	0.3	13.00	0.02
Substrate	87	0.3	11.2	0.5–3.0

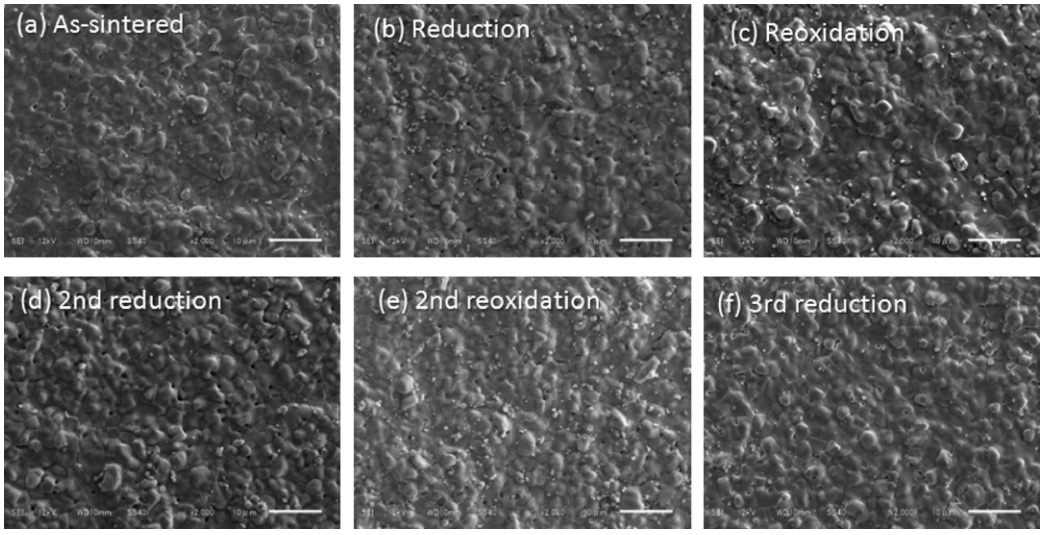

Fig. 2. SEM images of electrolyte surfaces of SIS-SOFCs without anode function layer after redox cycling.

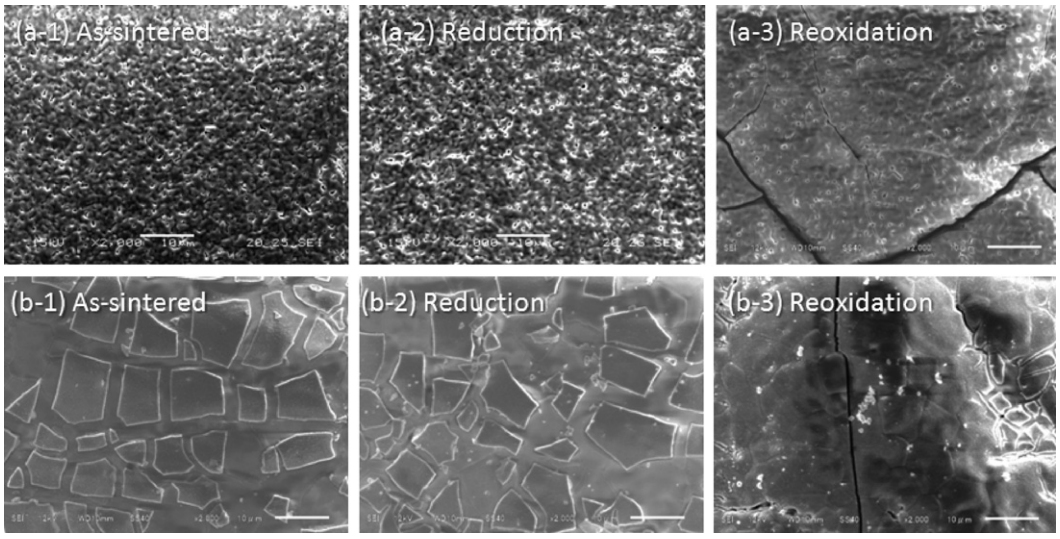

Fig. 3. SEM images of electrolyte surfaces of ASCs after redox reactions. The sample thicknesses are (a) 0.5 mm and (b) 3 mm.

3. Results and discussion

3.1. SEM images of SIS-SOFCs and ASCs

SEM images of the electrolyte surface of the SIS-SOFC without an AFL are shown in Fig. 2. The surface morphology retained almost the same structure after redox cycling. The electrolyte of the SIS-SOFC with an AFL showed the same morphology. However, some cracks were observed in the electrolyte surfaces of the ASCs after the reoxidation reaction, as shown in Fig. 3, and the SEM images of the electrolyte surfaces and cross-sectional views are shown in Fig. 4. The cracks in the electrolyte extended to the middle of the anode, and the behaviour of the ASCs was in agreement with results that have already been reported [12,14]. The cracks, which were

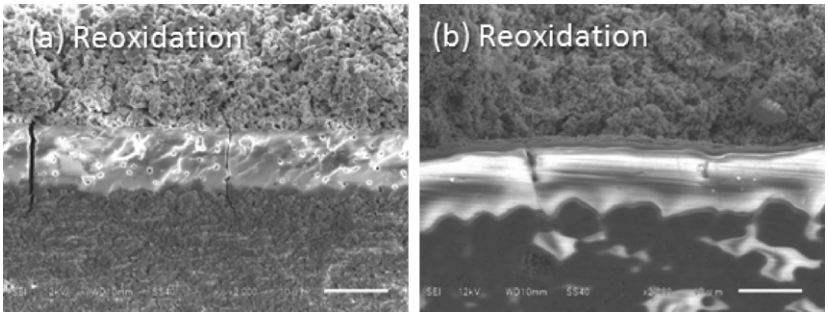

Fig. 4. Cross-sectional SEM images of ASCs of thicknesses (a) 0.5 mm and (b) 3 mm, after reoxidation.

observed in both kinds of ASCs, took place due to the expansion of the anode upon the reoxidation reaction. Zhang et al. [14] simulated the internal stresses in ASCs and reported that in order to maintain a low probability of failure, the anode thickness should be greater than 0.7 mm with an electrolyte thickness of 10 μm. The thickness of the electrolyte of the ASCs in this study was ~7–10 μm, and it was found that the redox process was enough to break down the structure of the ASC.

However, cracks in the electrolyte of the SIS-SOFC were not observed after redox cycling and the SIS-SOFC exhibited a high degree of tolerance for redox cycles. It was considered that not only the thin anode and thick substrate, but also the high chemical stability of the insulating material were responsible for this high tolerance.

3.2. X-ray residual stress measurement

The residual stresses in the electrolyte were measured at each redox step and the estimated results are shown in Table 2. The initial residual stress of 252.8 MPa in the electrolyte of the SIS-SOFC with AFL was obtained at room temperature, and this value remained almost constant upon redox cycling. Also, the residual stress of 353.1 MPa in the electrolyte of the SIS-SOFC without an AFL was relatively higher than that of the SIS-SOFC with an AFL. Because the amount of Ni in the AFL was smaller than in the anode, the dimensional change of the AFL was smaller than it was for the anode. Thus, the small residual stresses in the electrolyte were observed in the SIS-SOFC with an AFL. The residual stresses in the electrolyte of the ASCs were larger than that of the SIS-SOFC, and it was confirmed that these residual stresses were rapidly relaxed by the redox cycle. This relaxation upon reoxidation reaction was considered to be due to the cracks in the electrolyte that were observed in the SEM images. These results show that the residual stresses in the electrolyte of the SIS-SOFC can retain almost the same value when the anode expands upon reoxidation, and the high tolerance for redox cycling is attributed to the chemical stability of the supported substrate.

3.3. Numerical simulation results

The residual stresses in the electrolyte of the ASCs and the SIS-SOFCs at room temperature are shown in Fig. 5. The residual stresses in the electrolyte of the ASCs increased with the thickness of the anode substrate. The ASCs' residual stress at a thickness of 3 mm and 0.5 mm was about 588.0 MPa and 379.3 MPa, respectively. The estimated residual results in the ASCs demonstrated the same tendency and comparable values [14]. In addition, the experimental residual stresses of the ASC show the same tendency. The difference between the residual stress values in the experimental data and numerical data at a thickness of 0.5 mm was attributed to effect of the electrolyte thickness [13].

The residual stresses in the electrolyte of the SIS-SOFC without an AFL and with an AFL at room temperature were estimated

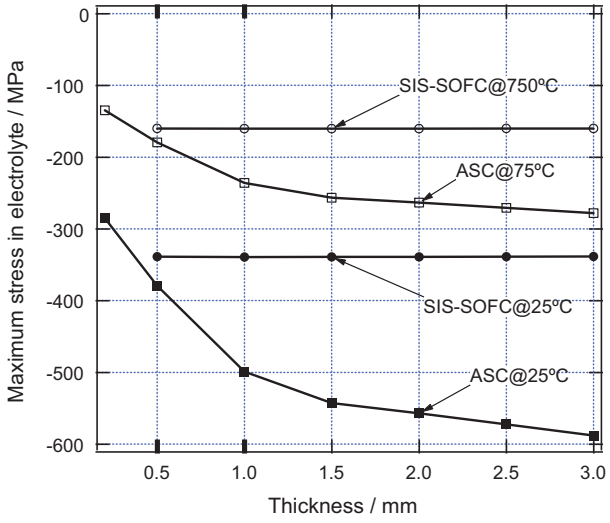

Fig. 5. Estimated residual stresses in electrolyte of SIS-SOFCs and ASCs at 25 °C and 750 °C.

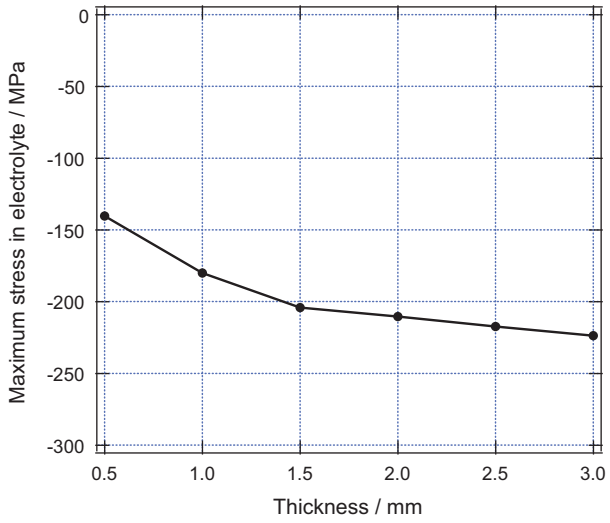

Fig. 6. SIS-SOFC substrate thickness dependencies of estimated residual stresses in electrolyte. The SIS-SOFC geometry is modelled from electrolyte and substrate.

to be ~339 MPa and 130.3 MPa, respectively. The residual stresses obtained by X-ray residual measurement were 353.1 MPa and 252.8 MPa, respectively. The residual stresses in the SIS-SOFC, which were simulated for various substrate thicknesses, are also shown in Fig. 5, and they show that the residual stresses were less affected by the thickness of the insulating substrate, but the residual stresses of the ASCs were very affected. As regards the residual stress behaviour, it was considered that the substrate and the elec-

Table 2
Residual stresses in electrolyte of SIS-SOFC and ASC at each redox step at room temperature.

Redox step	Electrolyte residual stress/MPa			
	ACS t = 0.5 mm	ACS t = 3 mm	SIS-SOFC without AFL	SIS-SOFC with AFL
As-sintered	−618.0 ± 30.2	−668.6 ± 32.5	−353.1 ± 8.9	−252.8 ± 38.3
1st reduction	−363.4 ± 20.9	−370.7 ± 31.6	−368.5 ± 10.9	−237.1 ± 11.7
1st reoxidation	−75.1 ± 37.9	−180.4 ± 18.2	−385.5 ± 4.7	−272.2 ± 27.7
2nd reduction	−46.2 ± 32.8	−128.0 ± 22.6	−403.2 ± 14.3	−235.6 ± 40.6
2nd reoxidation	–	–	−417.8 ± 6.1	−233.2 ± 45.0
3rd reduction	–	–	−410.5 ± 15.2	−224.1 ± 31.3
3rd reoxidation	–	–	−419.2 ± 27.1	−255.7 ± 33.9

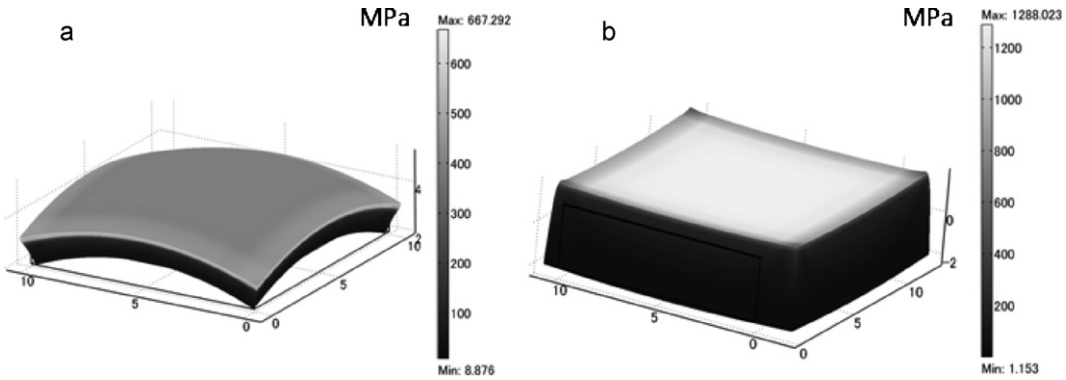

Fig. 7. Residual stresses in electrolyte of (a) SIS-SOFC and (b) ASC, after reoxidation reaction.

trolyte restrained the bending of the anode, and the area of the maximum residual stresses changed from the electrolyte to the anode. In fact, the residual stresses in the electrolyte were estimated from only the substrate and the electrolyte, and the residual stress were affected by the thickness of the surface, as shown in Fig. 6.

Next, we estimated the residual stresses that were affected by the redox reaction. First, residual stresses at 750 °C were estimated for various SOFCs. The residual stresses in the electrolyte of the SIS-SOFC were relaxed at high temperature; the results are shown in Fig. 5. Next, only the anode was expanded 50 μm in order to simulate the reoxidation reaction, giving results that are shown in Fig. 7(a). The residual stress in the electrolyte of 667.3 MPa was larger than the value before the reoxidation reaction.

A residual stress of 1288.0 MPa was obtained for the ASCs after reoxidation reaction, with the results shown in Fig. 7(b), and this value was greater than that for the SIS-SOFCs. The shape of the SIS-SOFC was a convex curve while the shape of the ASC was deformed to become a concave curve. The residual stress in the electrolyte of the SIS-SOFC retained the compressive stress, but the residual stress for the ASCs changed the tensile stress after reoxidation reaction. It was considered that the simulation results showed that the SIS-SOFC substrate could restrain the structural change and reduce the residual stresses in the electrolyte.

4. Conclusions

The residual stresses in the electrolyte of ASCs and SIS-SOFC were estimated using the X-ray stress measurement method and finite element method. The residual stress in the electrolyte of the SIS-SOFCs remained almost the same value during redox cycling. By contrast, the residual stress for the ASCs was relaxed and accompanied by some crack formation upon reoxidation. This high redox tolerance is regarded as being due to the insulating substrate, which restrains the expansion of the anode. It is considered that the insertion of a chemically stable layer can effectively enhance redox tolerance.

References

[1] E. Tang, D. Prediger, M. Pastula, B. Borglum, in: J. Mizusaki, S.C. Singhal (Eds.), Solid Oxide Fuel Cells 9 (SOFC-IX), Quebec, Canada, Electrochem. Soc. (2005) 89–97.
[2] J. Love, S. Amarasinghe, D. Selvey, X. Zheng, L. Christiansen, in: S. Singhal, H. Yokokawa (Eds.), Solid Oxide Fuel Cells 11 (SOFC-XI), Vienna, Austria, ECS Trans. (2009) 115–124.
[3] S. Kluge, O. Posdziech, B. Mai, J. Lawrence, in: S. Singhal, H. Yokokawa (Eds.), Solid Oxide Fuel Cells 11 (SOFC-XI), Vienna, Austria, ECS Trans. (2009) 247–256.
[4] T. Klemens, M. Mogensen, J. Am. Ceram. Soc. 90 (2007) 3582–3588.
[5] M. Pihlatie, A. Kaiser, M. Mogensen, Solid State Ionics 180 (2009) 1100–1112.
[6] J. Laurencin, G. Delette, O. Sicardy, S. Rosini, F. Lefebvre-Joud, J. Power Sources 195 (2009) 2747–2753.
[7] T. Klemens, C. Chung, P. Larsen, M. Mogensen, J. Electrochem. Soc. 152 (2005) A2186–A2192.
[8] D. Waldbillig, A. Wood, D. Ivey, J. Electrochem. Soc. 154 (2007) B133.
[9] A. Wood, M. Pastula, D. Waldbillig, D. Ivey, J. Electrochem. Soc. 153 (2006) A1929.
[10] S. Tao, J. Irvine, Nat. Mater. 2 (2003) 320–323.
[11] J. Malzbender, W. Fischer, R. Steinbrech, J. Power Sources 182 (2008) 594–598.
[12] A. Atkinson, B. Sun, Mater. Sci. Technol. 23 (2007) 1135–1143.
[13] H. Yakabe, Y. Baba, T. Sakurai, Y. Yoshitaka, J. Power Sources 135 (2004) 9–16.
[14] T. Zhang, Q. Zhu, W. Huang, Z. Xie, X. Xin, J. Power Sources 182 (2008) 540–545.
[15] K. Fujita, Y. Matsuzaki, H. Yakabe, S. Yamashita, K. Ogasawara, T. Sakurai, Proceedings of 4th international ASME Conference on Fuel Cell Science Engineering and Technology (FuelCell 2006), ASME, Irvine, CA, USA, June 19–21, 2006, 2006, on CD.
[16] M. Koi, S. Yamashita, Y. Matsuzaki, in: K. Eguchi, J. Mizusaki, S. Singhal, Yokokawa H. (Eds.), Solid Oxide Fuel Cells 10 (SOFC-X), Nara, Japan, ECS Trans. (2007) 235–243.
[17] Y. Matsuzaki, M. Koi, S. Yamashita, Proceedings of 2nd European Fuel Cell Technology and Applications Conference (EFC 2007), Rome, Italy, December 11–14, 2007, pp. 153–154.
[18] K. Horiuchi, T. Somekawa, Y. Matsuzaki, M. Nishihara, Proceedings of 2nd European Fuel Cell Technology and Applications Conference (EFC 2007), Rome, Italy December 11–14, 2007, pp. 155–156.
[19] T. Somekawa, K. Horiuchi, Y. Matsuzaki, M. Nishihara, Proceedings of 31st international Cocoa Beach Conference & Exposition on Advanced Ceramics & Composites, Daytona Beach, FL, USA, January 21–28, 2008, pp. 167–168.
[20] J. Van Herle, D. Perednis, K. Nakamura, S. Diethelm, M. Zahid, A. Aslanides, T. Somekawa, Y. Baba, K. Horiuchi, Y. Matsuzaki, J. Power Sources 182 (2008) 389–399.
[21] K. Fujita, T. Somekawa, K. Horiuchi, Y. Matsuzaki, J. Power Sources 193 (2009) 130–135.
[22] K. Nakamura, T. Somekawa, Y. Baba, K. Horiuchi, Y. Matsuzaki, M. Yoshimoto, J. Ceram. Soc. Jpn. 117 (2009) 166–170.
[23] Y. Matsuzaki, Y. Baba, T. Ogiwara, H. Yakabe, Proceedings of 5th European SOFC Forum, Lucerne, July 1–5, 2002, pp. 776–783.
[24] Y. Matsuzaki, Y. Baba, T. Sakurai, Solid State Ionics 174 (2004) 81–86.
[25] A. Selcuk, A. Atkinson, J. Am. Ceram. Soc. 83 (2000) 2029–2035.
[26] A. Atkinson, A. Selcuk, Solid State Ionics 134 (2000) 59–66.